

## Possible Origin of Anisotropic Resistive Hysteresis in the Vortex State of Untwinned $\text{YBa}_2\text{Cu}_3\text{O}_7$ Single Crystals

W. Jiang,<sup>1</sup> N.-C. Yeh,<sup>1</sup> D. S. Reed,<sup>1</sup> U. Kriplani,<sup>1</sup> and F. Holtzberg<sup>2</sup>

<sup>1</sup>*Department of Physics, California Institute of Technology, Pasadena, California 91125*

<sup>2</sup>*IBM, Thomas J. Watson Research Center, Yorktown Heights, New York 10598*

(Received 29 July 1994)

The origin of resistive hysteresis in untwinned  $\text{YBa}_2\text{Cu}_3\text{O}_7$  single crystals is investigated for time scales from 1 to  $10^3$  sec and for frequencies from  $10^1$  to  $10^6$  Hz. The absence of resistive “subloops” upon partial heating and cooling, the lack of time dependence, and the decreasing hysteresis with the increasing angle between the applied magnetic field and crystalline  $c$  axis suggest that the hysteresis is not a direct evidence of a first-order vortex-solid melting transition. A current-induced nonequilibrium effect is proposed as the possible origin for the hysteresis.

PACS numbers: 74.60.Ec, 74.25.Dw, 74.60.Ge, 74.72.Bk

Recent theoretical work using Monte Carlo simulations [1] has provided convincing evidence for a first-order vortex-solid melting transition in “very clean” high-temperature superconductors by demonstrating hysteretic behavior of the internal energy. Subsequent observation of resistive hysteresis [2–4] in the vortex state of untwinned  $\text{YBa}_2\text{Cu}_3\text{O}_7$  single crystals has been commonly accepted as the experimental evidence for the first-order transition. However, it remains an open question whether a nonthermodynamic quantity such as the resistivity should follow the same hysteretic behavior as the internal energy. If the resistive hysteresis is indeed associated with the occurrence of a first-order phase transition, one would then expect that upon partial heating and cooling cycles partial hysteresis loops would also be present due to the finite latent heat and solidification time. Furthermore, if the temperature width of the hysteresis  $\Delta T_{\ell p}$  is proportional to the latent heat as suggested [5], one would expect  $\Delta T_{\ell p}$  in anisotropic  $\text{YBa}_2\text{Cu}_3\text{O}_7$  single crystals to increase with increasing angle ( $\theta$ ) between the applied magnetic field and the crystalline  $c$  axis, because the melting temperature ( $T_M$ ) and therefore the latent heat increases with  $\theta$ . However, to date no detailed dependence of the resistive hysteresis on time, frequency, and magnetic field orientation has been investigated. Aiming at these issues, we present in this Letter experimental studies of the anisotropic resistive hysteresis in untwinned  $\text{YBa}_2\text{Cu}_3\text{O}_7$  single crystals over three decades of time and six decades of frequency. The absence of resistive “subloops” upon partial heating and cooling, the lack of time dependence, as well as the *decreasing* hysteresis with increasing melting temperatures, strongly suggests that the resistive hysteresis is not directly associated with a first-order phase transition. A current-induced nonequilibrium effect near the onset of vortex dissipation is proposed to account for the occurrence of the hysteresis.

The sample studied in this work is an untwinned  $\text{YBa}_2\text{Cu}_3\text{O}_7$  single crystal with dimensions of  $0.5 \text{ mm} \times 0.5 \text{ mm} \times 20 \text{ }\mu\text{m}$ . The high quality of the sample is

demonstrated by the high superconducting transition temperature  $T_c = 93.18 \pm 0.03 \text{ K}$  and the low normal-state  $a$ -axis resistivity  $\rho_n = 25 \text{ }\mu\Omega \text{ cm}$  at  $T_c$ . Three types of electrical transport measurements are performed with the use of a standard four-terminal method. The first measurement is that of the linear resistivity ( $\rho$ ) as a function of the temperature ( $T$ ) by using the lock-in technique with four different current densities at 27 Hz. The voltage resolution is 1 nV, and temperature stability is within  $\pm 1 \text{ mK}$ . The second experiment involves measuring isotherms of the ac impedance as a function of the applied current frequency ( $f$ ), from 100 Hz to 1 MHz. The third experiment measures dc current-voltage characteristics. All measurements are performed in applied magnetic fields ( $H$ ) from 1 to 90 kOe and for angles ( $\theta$ ) from  $0^\circ$  to  $90^\circ$ . The applied current density  $\mathbf{J}$  is always transverse to  $\mathbf{H}$  and  $\mathbf{J} \perp \hat{c}$ .

Hysteresis behavior is observed in the  $\rho$  vs  $T$  measurements for  $H \geq 10 \text{ kOe}$  and  $\theta < 90^\circ$ . Shown in Figs. 1(a) and 1(b) are the representative data taken at  $H = 50$  and  $70 \text{ kOe}$  and for  $\theta = 0^\circ$ . At each constant magnetic field, the temperature is ramped in steps of 5 mK. At each step, the temperature is monitored for  $\sim 3 \text{ min}$  to ensure the temperature stability before the data are taken. The hysteresis width  $\Delta T_{\ell p}$  for a given  $H$  and  $\theta$  is defined as the temperature width at the top of the resistive loop. The magnetic field dependence of  $\Delta T_{\ell p}$  for  $\mathbf{H} \parallel \hat{c}$  is shown in the inset of Fig. 1(b). A peak in  $\Delta T_{\ell p}$  is found at  $\sim 70 \text{ kOe}$ , consistent with previous reports in Ref. [2].

To investigate whether the resistive hysteresis is directly associated with the latent heat of a first-order melting transition, consider a hysteresis loop  $A \rightarrow B \rightarrow C' \rightarrow A' \rightarrow B' \rightarrow C \rightarrow A$  arising from superheating and supercooling vortices so that the bulk melting temperature  $T_M$  is between  $T_A$  and  $T_B$ , as shown schematically in the inset of Fig. 2. A partial heating and cooling cycle which follows the history of  $A \rightarrow B \rightarrow C \rightarrow A$  would result in a subloop indicated by the dashed line, because during the cooling process from  $T_B$  to  $T_A$  the liquid regions have to dissipate excess latent

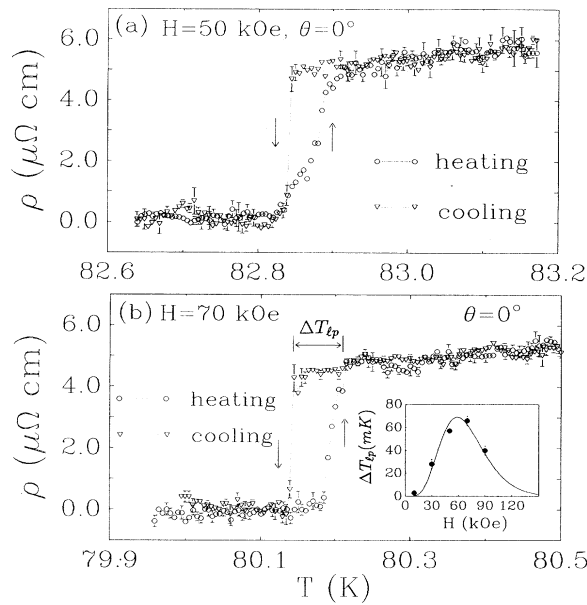


FIG. 1. Representative data of the relative hysteresis  $\rho$  as a function of temperature  $T$ . (a)  $H = 50 \text{ kOe}$  and  $\theta = 0^\circ$ . (b)  $H = 70 \text{ kOe}$  and  $\theta = 0^\circ$ . The inset shows the temperature width of the hysteresis  $\Delta T_{lp}$  as a function of the magnetic field  $H$ .

heat before complete solidification. Therefore the resistivity would not immediately reduce to that of the heating process  $A \rightarrow B$ . Similarly, for a partial cooling and heating cycle following the history of  $A' \rightarrow B' \rightarrow C' \rightarrow A'$ , a subloop indicated by the dashed line is expected, because once some liquid regions solidified they would not melt immediately upon the heating process  $B' \rightarrow C'$ . However, our experimental data for all  $H$  and  $\theta$  do not show any evidence of subloops, as exemplified in Fig. 2 for  $H = 50 \text{ kOe}$  and  $\theta = 0^\circ$ , contradicting the assumption of first-order related resistive hysteresis.

Next we consider the time dependence of the hysteresis. If the hysteresis is associated with conventional superheating and supercooling, when the system is warmed up from  $T_A$  to  $T_B$  and kept at  $T_B$  for a sufficiently long time, a larger area of the vortex solid melts, so that the resistivity at  $T_B$  increases with increasing time. Similarly, if one follows the supercooling curve  $A' \rightarrow B'$  and keeps the system at  $T_{B'}$  for a long time, the resistivity decreases with increasing time because larger regions of the liquid solidify. Similar time-dependent resistivity is also expected for a "first-order glass transition" in systems with a broad distribution of metastable states [5], because the longer vortices stay in the glass state the lower the metastable states they fall into, giving rise to smaller resistivity with increasing time. However, all experimental data taken at  $T_B$  and  $T_{B'}$  for various scans and with wait times ranging from 1 to  $10^3$  sec show no visible changes in the resistivity. The lack of time dependence again suggests that the hysteresis is not directly related to the latent heat.

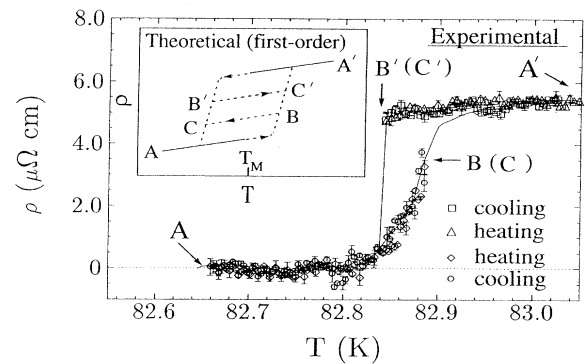


FIG. 2. History and time dependence of the resistivity hysteresis. The solid curves are the experimental data given in Fig. 1(a), and the data points shown are taken for partial heating and cooling cycles. The inset is a schematic hysteresis and the corresponding subloops based on the assumption of a first-order phase transition.

In addition to investigating subloops and time dependence, it is also important to understand the anisotropic behavior of the resistive hysteresis. According to the first-order glass transition model [5], the latent heat absorbed during the melting process is proportional to  $T_M$ . Since  $T_M$  increases with increasing  $\theta$  in  $\text{YBa}_2\text{Cu}_3\text{O}_7$  single crystals, one expects  $\Delta T_{lp}$  to also increase with  $\theta$  if  $\Delta T_{lp}$  is proportional to the latent heat. However, as shown in Fig. 3,  $\Delta T_{lp} \rightarrow 0$  as  $\theta \rightarrow 90^\circ$ , contrary to the expected increasing  $\Delta T_{lp}(\theta)$ . Such angular dependence cannot be straightforwardly explained by the first-order melting model.

To find out whether pinning is responsible for the above experimental observation, we perform frequency dependent measurements of  $\Delta T_{lp}$  by applying ac transport currents to the sample. Figure 4 shows  $\Delta T_{lp}$  vs  $f$  data for  $\theta = 0^\circ$  and  $H = 50$  and  $70 \text{ kOe}$ . We note that the data do not follow the typical frequency dependence for a vortex energy barrier  $U \sim k_B T \ln[1/(2\pi f\tau)]$ , if  $\Delta T_{lp} \propto U$  is assumed, and  $\tau$  is a characteristic relaxation time [6].

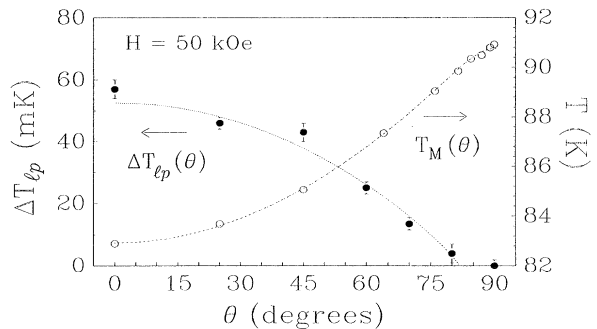


FIG. 3. The angular dependence of the resistive hysteresis width  $\Delta T_{lp}(\theta)$  and the melting temperature  $T_M(\theta)$  for  $H = 50 \text{ kOe}$ . The dotted line is the theoretical fitting for the angular dependent  $\Delta T_{lp}(\theta)$  by using Eq. (3), and the dashed line is the fitting for the angular dependent  $T_M(\theta)$  by using Eq. (4).

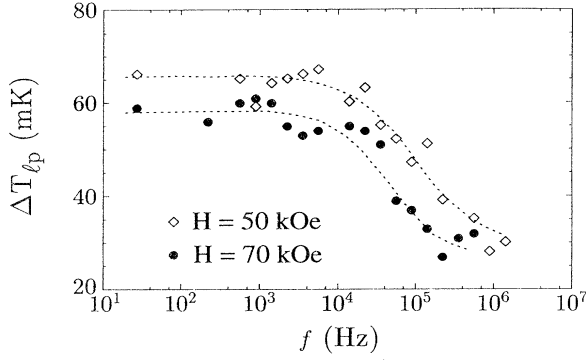


FIG. 4. The frequency dependence of the hysteresis width  $\Delta T_{\ell_p}(f)$  for  $\theta = 0^\circ$ ;  $H = 50$  and  $70$  kOe.

Instead,  $\Delta T_{\ell_p}$  is nearly independent of the frequency up to  $f \approx 3 \times 10^4$  Hz and then decreases rapidly until  $f \sim 10^6$  Hz.

Another important issue to be addressed is the sharpness of the resistive transition. We find that although the resistive transition for  $\theta = 0^\circ$  and  $H \geq 10$  kOe is always very sharp, typically  $< 10^{-1}$  K, the linear resistivity near the onset becomes more gradual with increasing  $\theta$ . In particular, for data taken at  $\theta = 90^\circ$  and for all fields, the onset of resistivity is such that the current-voltage characteristics follow the critical scaling behavior for a second-order  $XY$ -like transition [7,8], consistent with recent experimental observation [3] and the theoretical interpretation of a smectic crystal to vortex-liquid transition near  $\theta \approx 90^\circ$  [9].

In view of all the experimental results given above, we propose a current-induced nonequilibrium effect as a possible scenario for the occurrence of resistive hysteresis. Suppose that the untwinned samples are nearly free of defects so that the pinning potential ( $U_p$ ) is less significant than the elastic energy near the vortex-solid melting temperature  $T_M$ . As the sample is cooled down from the vortex-liquid state and a current is applied for resistive measurements, vortices are driven by the Lorentz force until the local shear elastic energy becomes finite. The shear energy per flux line below  $T_M$  can be expressed by  $U_s = c_{66} \xi_s^2 L_c$  [5], where  $c_{66}$  is the shear modulus,  $\xi_s$  is the superconducting coherence length, and  $L_c$  the longitudinal vortex correlation length. We note that  $c_{66} = 0$  at  $T_M$ , although the total elastic energy is still finite due to the finite tilt energy ( $c_{44} \neq 0$ ). This definition is different from the conventional one [10] which asserts  $c_{66} \neq 0$  until  $H_{c2}(T)$ , so that the presence of a vortex-liquid state is implicitly neglected. Since vortices are moving with an initial velocity  $v$  upon cooling, where  $v \propto J$  is the flux-flow velocity, the onset of finite  $c_{66}$  would not be sufficient to impede the vortex motion immediately. Thus, the system “supercools” until  $U_s$  exceeds the work ( $W$ ) done by the current. That is,

$$U_s = c_{66} \xi_s^2 L_c \approx W = (J - J_c) \Phi_0 \xi_s L_c \quad \text{at } T = (T_M - \Delta T_{\ell_p}), \quad (1)$$

where  $\Phi_0$  is the flux quantum and  $J_c$  is the critical current density. Once  $U_s \geq W$ , the resistivity begins to drop precipitously. On the other hand, if the system is warmed up from the vortex-solid state, the initial vortex velocity is smaller than the flux-flow velocity, so that the resistivity (which is proportional to  $v$ ) increases smoothly and stays below that of the cooling curve until  $U_s \rightarrow 0$ .

To test the scenario quantitatively, consider the following expression for the shear modulus:

$$c_{66}(T \leq T_M, H) = c_{66}^0(H) \{1 - [T/T_M(H)]\}^{\nu_s}, \quad (2)$$

so that  $c_{66} = 0$  at  $T_M$ , and  $c_{66}^0(H)$ , as well as  $\nu_s$ , are to be determined empirically. Thus,  $\Delta T_{\ell_p}$  can be derived from Eqs. (1) and (2), which yields

$$\Delta T_{\ell_p}(H, \theta) = T_M(H, \theta) \left\{ \frac{(J - J_c) \Phi_0}{c_{66}^0(H, \theta) \xi_s} \right\}^{1/\nu_s}. \quad (3)$$

By applying Eq. (3) to the  $\Delta T_{\ell_p}$  vs  $H$  data for  $\theta = 0^\circ$ , and assuming  $J_c$  is independent of  $H$ , we obtain the fitting curve for  $c_{66}^0(H, 0^\circ)$ , and the fitting parameter  $\nu_s \approx 1.3$ . The corresponding fitting curve of  $\Delta T_{\ell_p}(H, 0^\circ)$  vs  $H$  is shown by the solid line in the inset of Fig. 1(b). We note that, for  $H \leq 70$  kG,  $\Delta T_{\ell_p}$  increases with  $H$ , indicating a decreasing  $c_{66}^0(H, 0^\circ)$  which is consistent with a decreasing superconducting order parameter and therefore smaller elasticity [10]. However, our observation of decreasing  $\Delta T_{\ell_p}$  for  $H > 70$  kG and the report [2] of  $\Delta T_{\ell_p} \rightarrow 0$  at  $H \sim 100$  kG suggest an increase in either  $c_{66}^0$  or  $J_c$  above  $H \sim 100$  kG. This finding may be attributed to the increasing importance of pinning when the flux line separation in higher fields becomes comparable to the average distance between point defects [2]. However, this issue still awaits further theoretical investigations.

To examine the angular dependence of  $\Delta T_{\ell_p}$ , we note that the angular dependence of  $c_{66}^0$  is given by the hard-axis shear modulus of the vortex lattice [11,12],  $c_{66}^0(H, \theta) = \varepsilon_\theta^{-1} c_{66}^0(H, 0^\circ)$ , because  $\mathbf{J} \perp \mathbf{H}$  and  $\mathbf{J} \perp \hat{\mathbf{c}}$  for all  $\theta$  so that the Lorentz force is always along the hard axis. Here  $\varepsilon_\theta \equiv \sqrt{\cos^2 \theta + \varepsilon^2 \sin^2 \theta}$ , and  $\varepsilon^{-2} \approx 60$  is the mass anisotropy ratio [13]. The angular-dependent melting temperature  $T_M(H, \theta)$  can be obtained by using the relation for the melting field  $H_M(\theta) = \varepsilon_\theta^{-1} H_M(0^\circ)$  [14] and the empirical relation  $H_M(T) = H_M^0 [1 - (T/T_c)]^{2\nu_0}$  with  $2\nu_0 \approx 1.4$  from fitting the experimental data. Thus, we obtain

$$T_M(H, \theta) = T_c [1 - (H \varepsilon_\theta / H_M^0)^{1/(2\nu_0)}], \quad (4)$$

which agrees well with the  $T_M(H, \theta)$  vs  $\theta$  data in Fig. 3. Using  $\xi_s^2(T) = \xi_s^2(0) [1 - (T/T_c)]^{-1}$ ,  $\xi_s(0) \approx 20$  Å,  $J = 0.27$  A/cm<sup>2</sup>,  $J_c(0^\circ) \approx 0.2J$ , and the approximation  $J_c(\theta) = \varepsilon_\theta^{-1} J_c(0^\circ)$ , we find that the angular dependence of  $\Delta T_{\ell_p}(\theta)$  in Eq. (3) is consistent with the experimental data, as shown by the dotted curve in Fig. 3.

Another stringent test for our model is to consider the current dependence of  $\Delta T_{\ell_p}$ . If the applied current density is too high, vortex motion occurs well below the thermodynamic melting temperature  $T_M$ . Therefore

the condition  $U_s \approx W$  in Eq. (1) cannot be satisfied near  $T_M$ , the resistive transition broadens, and hysteresis vanishes. On the other hand, if the applied current density is so small that  $(J - J_c)\Phi_0 \ll c_{66}^0 \xi_s$ , then  $\Delta T_{\ell p} \rightarrow 0$  according to Eq. (3). It is therefore not surprising that the anisotropic hysteresis width  $\Delta T_{\ell p}$  decreases rapidly when  $\theta \rightarrow 90^\circ$ , because both  $c_{66}^0(\theta)$  and  $J_c(\theta)$  increase substantially. Another corollary of our model is that for comparable values of  $(J - J_c)\Phi_0$  and  $(c_{66}^0 \xi_s)$ , the cooling branch of the resistivity would move slightly towards lower temperatures with increasing  $J$ , because vortices had to supercool more to compensate for the larger driving force of the currents. This argument predicts an increase in  $\Delta T_{\ell p}$  with a small increase of  $J$  according to Eq. (3), and is confirmed by the data in Fig. 5 for three different densities  $J = 0.27, 2.70,$  and  $9.99 \text{ A/cm}^2$  and for  $H = 70 \text{ kG}$ . Similar results for  $H = 50 \text{ kG}$  and  $J = 0.27, 9.99,$  and  $16.55 \text{ A/cm}^2$  are also shown in the inset of Fig. 5. We note that for both magnetic fields the heating branches broaden with increasing  $J$ , in contrast to the nearly constant width of the cooling branches. Furthermore, the temperatures where the heating curves begin to drop precipitously remain the same for all current densities, whereas those for the cooling curves decrease with increasing  $J$ . Thus,  $\Delta T_{\ell p}$  increases with  $J$ , consistent with Eq. (3) and the report in Ref. [3].

The above scenario may also be applicable to the frequency dependence of  $\Delta T_{\ell p}(f)$  in Fig. 4, because  $c_{66}$  becomes effectively "stiffer" with the increasing frequency of the ac current, so that  $\Delta T_{\ell p}$  decreases. However, quantitative understanding of the frequency dependence requires better knowledge of the dispersion relation for  $c_{66}(f)$ . Finally, we notice the importance of small  $J_c$ , small  $\xi_s$ , and high  $T_M$  for the occurrence of resistive hysteresis. The latter two conditions are unique features of high-temperature superconductors, and the first

is unique for weak-pinning samples such as untwinned  $\text{YBa}_2\text{Cu}_3\text{O}_7$  single crystals.

Although the proposed current-induced nonequilibrium effect can successfully explain the magnetic field, current, frequency, and angular dependence of the resistive hysteresis in untwinned  $\text{YBa}_2\text{Cu}_3\text{O}_7$  single crystals, it is important to realize that this model does not distinguish whether the vortex-solid melting transition is first or second order. The only conclusions we can draw from the investigations are that vortices are weakly pinned, and that the resistive hysteresis occurs below the thermodynamic melting temperature. The hysteresis itself is neither a sufficient nor a necessary condition for a first-order melting transition, and its width is not directly related to the latent heat. Although the weak pinning and sharp resistive transition in the vortex state of untwinned  $\text{YBa}_2\text{Cu}_3\text{O}_7$  single crystals are very suggestive of a first-order melting transition, this issue can only be unambiguously settled with measurements of thermodynamic quantities such as specific heat or magnetization.

The authors are grateful to Professor R. Huebener and Professor T.A. Tombrello for stimulating discussions. This work was jointly supported by ONR Grant No. N00014-91-J-1556, the David and Lucile Packard Foundation, and NASA/OACT.

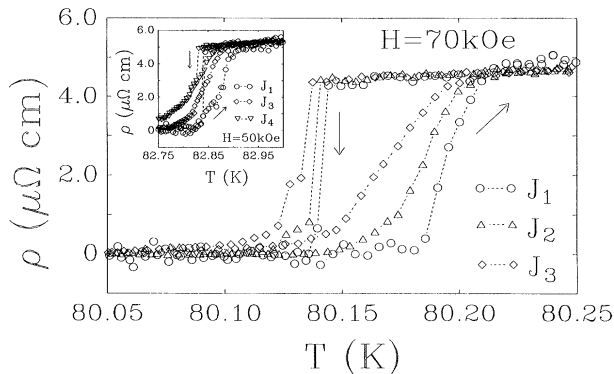


FIG. 5. The current dependence of the resistive hysteresis for  $H = 70 \text{ kOe}$ , and  $\theta = 0^\circ$  is shown for three different current densities  $J_1 = 0.27, J_2 = 2.70,$  and  $J_3 = 9.99 \text{ A/cm}^2$ . The inset shows similar results for  $H = 50 \text{ kOe}$ ,  $\theta = 0^\circ$ , and  $J = J_1, J_3, J_4 (= 16.55 \text{ A/cm}^2)$ .

- [1] R. E. Hetzel, A. Sudbo, and D. A. Huse, Phys. Rev. Lett. **69**, 518 (1992).
- [2] H. Safar *et al.*, Phys. Rev. Lett. **69**, 824 (1992); **70**, 3800 (1993).
- [3] W. K. Kwok *et al.*, Phys. Rev. Lett. **69**, 3370 (1992); **72**, 1088 (1994); **72**, 1092 (1994).
- [4] M. Charalambous *et al.*, Phys. Rev. Lett. **71**, 436 (1993). In this work a weakly time-dependent  $c$ -axis resistive hysteresis is reported on a twinned  $\text{YBa}_2\text{Cu}_3\text{O}_7$  single crystal with a different experimental configuration of  $\mathbf{J} \parallel \mathbf{c}$  and  $\mathbf{H} \parallel ab$  plane..
- [5] V. B. Geshkenbein, L. B. Ioffe, and A. L. Larkin, Phys. Rev. B **48**, 9917 (1993).
- [6] C. J. van der Beek, V. B. Geshkenbein, and V. M. Vinokur, Phys. Rev. B **48**, 3393 (1993).
- [7] N.-C. Yeh *et al.*, Phys. Rev. B **47**, 6146 (1993); Mater. Res. Soc. Symp. Proc. **275**, 169 (1992); Phys. Rev. B **45**, 5645 (1992).
- [8] D. S. Reed *et al.*, Phys. Rev. B **47**, 6150 (1993); Mater. Res. Soc. Symp. Proc. **275**, 413 (1992).
- [9] L. Balents and D. R. Nelson, Phys. Rev. Lett. **73**, 2618 (1994).
- [10] E. H. Brandt, J. Low Temp. Phys. **26**, 709 (1977); **26**, 735 (1977).
- [11] V. G. Kogan and L. J. Campbell, Phys. Rev. Lett. **62**, 1552 (1989).
- [12] G. Blatter, V. B. Geshkenbein, and A. I. Larkin, Phys. Rev. Lett. **68**, 875 (1992).
- [13] R. G. Beck *et al.*, Phys. Rev. Lett. **68**, 1594 (1992).
- [14] G. Blatter *et al.*, Rev. Mod. Phys. (to be published).